International Journal of Signal Processing, Image Processing and Pattern Recognition
Vol.9, No.10, (2016), pp.57-68
http://dx.doi.org/10.14257/ijsip.2016.9.10.06

Wood Surface Defect Image Segmentation Method based on Canny Operator and GGAC Model of Reaction Diffusion Equation

Zhang Xianhong[1] and Zhang Chunrui[2*]

[1]Electrical Engineering Department, Northeast Forestry University, China
[2]Department of mathematical, Northeast Forestry University, China
[1]haozhangxianhong@hotmail.com, [2]110464001@qq.com

Abstract

GGAC is an improvement based on geodesic active contour model (GAC). GGAC model is a widely used method for image segmentation. But, it will be difficult to achieve satisfactory segmentation results to the texture, uneven structure, edge particles, weak edge and other features of the wood surface image. Therefore, the author proposes a segmentation method that integrates the improved Canny edge detection result integrated into the improved GGAC model redrawing boundary stop function, and uses the improved variational level set method to achieve the numerical solution. The algorithm has reduced the choice sensitivity to the initial contour and enhanced the scalability, which can make the profile curve converge to defect edges more rapidly, avoid the local optimum, and improve segmentation effects of weak edges and uneven image. The results are clearer, more consistent and real-time. It has provided a more effective way to segment the wood surface defects, and broadened the application scope of Canny operator and an improved geodesic active contour model.

Keywords: *P-M model, Canny operator, GGAC model, Image segmentation*

1. Introduction

Wood surface defects affect the appearance and quality of the wood products and reduce the value of the wood. Therefore, the effective segmentation of defects image on the wood surface can increase the volume ratio of wood and economic efficiency. Domestic and foreign scholars have carried out extensive researches on the segmentation methods of the wood defect images. L. Wang[1], *et. al.*, proposed the wood surface defect image segmentation method based on Gabor transform, but the segmentation accuracy only reaches 98.29%. X. B. Bai[2], *et. al.*, proposed the wood surface defect image segmentation method based on Markov random field, which has effectively segmented the defect image of the wood surface, but still did not segment the knot image to the full extent. Jianjun Yuan [3], *et. al.*, proposed An improved geodesic active contour model with points distance and gray intensity is proposed in this paper for the segmentation of images, in which, the proposed model extends the traditional geodesic active contour model and correctly segments objects with lower contrast. However, this method is not effective enough for edge detection of images with weak edges.

In order to better extract wood defect image having a weak boundary, the paper combines advantages of Canny edge detection algorithm with the advantages of GGAC model extraction algorithm, and proposes a wood surface defect image segmentation method based on Canny operator of reaction-diffusion equations and

*Corresponding Author

ISSN: 2005-4254 IJSIP

GGAC model [4]. J. S. Shen [5], *et. al.*, had made a similar approach for applying to GAC mode extraction of the water line, but local minimum value problem of the GAC model was prone to occur boundary leakage, and the traditional Canny operator also has many deficiencies. Therefore, compared with the conventional method, the improved method has not only improved segmentation method, but also is more suitable for applying to the wood surface defect image with a weak boundary. When using the improved variational level set method [6] for the numerical realization, the algorithm is simple, and the amount of calculation is also small, hence one can realize real time and effective segmentation in image processing. Through simulation experiments, the author has obtained satisfactory segmentation results. This method is a breakthrough in processing of defect image on wood surface with a weak boundary, and also has broadened the application scope of the GAC model.

2. Canny Operator and GGAC Model Improvement

2.1. Canny Operator Improvement

The Canny operator is an edge detection algorithm proposed by John Canny[7] in 1986. Canny converted the edge detection problem into extreme value of unit function detection. Canny operator is a good edge detection operator. In the traditional Canny algorithm, it uses Gaussian filter for filtering. The main purpose of image smoothing filtering is to improve the signal noise ratio (SNR), and eliminate noises, but it will cause excessive smoothness the process of Gaussian smoothing. Edge will be smoothed out as a high-frequency components, making some edges become the graded edges, so that when the non-maxima is under suppression, the graded edge will be lost. In 1990, Perona and Malik[8] proposed anisotropic diffusion model, which can better smooth the images, remove noises, and also maintain the edge features.

In P-M model, $u_0(x, y)$ is the raw gray scale image as the initial condition, and t is the time variable. ∇ is the gradient operator, div is the divergence operator; $c(x, y, t)$ means diffusion coefficient, $|\nabla u|$ is the gradient magnitude[8], so Eq. (1) as[3]:

$$\begin{cases} \dfrac{\partial u(x, y, t)}{\partial t} = div\left[g(|\nabla u|)\nabla u\right] \\ u\,|_{t=0} = u_0 \end{cases} \tag{1}$$

The partial differential equation can be understood in this way: the original image u_0 in the definition domain serves as a medium, which diffuses at a non-constant velocity on the image, and its diffusion region gradually becomes a series of smooth images u_t. As non-negative monotone decreasing function, diffusion function $g(x)$ provides the degree of diffusion, and when $x \to \infty$, $g(x) \to 0$. This ensures that the image would stop the diffusion in the edge area to maintain the edge information.

For an image, $|\nabla u|$ is usually very large and $g(|\nabla u|)$ is very small at the edges with small degree of diffusion; in a flat area, $|\nabla u|$ is small but $g(|\nabla u|)$ is large, hence degree of diffusion becomes larger, so that one can selectively smooth the image: the edges get less smoothed, but become much smoother at flat area, so as to de-noise and maintain the edges[9].Two $g(x)$ functions are given in the P-M model as Eq. (2) and Eq. (3)[8]:

$$g(x) = e^{-\left(x/k\right)^2} \tag{2}$$

$$g(x) = \frac{1}{1 + \left(x/k\right)^2} \tag{3}$$

Here, k is a given constant. In Figure 1, when k=1, to observe the changes of the curve of the function in the case of -4<=x<=4. As can be seen from Figure 1, $|\nabla u|$ gradually increase and gets close to the edge, the velocity Eq. (2) close to zero is faster than Eq. (3). The excessive high velocity for being close to zero will rapidly slow down the diffusion near the edge of the area, so that the smoothing degree is not enough, and the noise removal effect becomes weaker, so people usually use diffusion function Eq. (3), however with respect to Eq. (2), Eq. (3) has a larger smoothing degree at a small portion of the flat area $|\nabla u|$, which will easily lead to an over smoothing; moreover, the velocity close to zero will make the image subject to the diffusion of neighbor pixels at a very large gradient on the image edge , resulting in blurred edges and even destroyed edges.

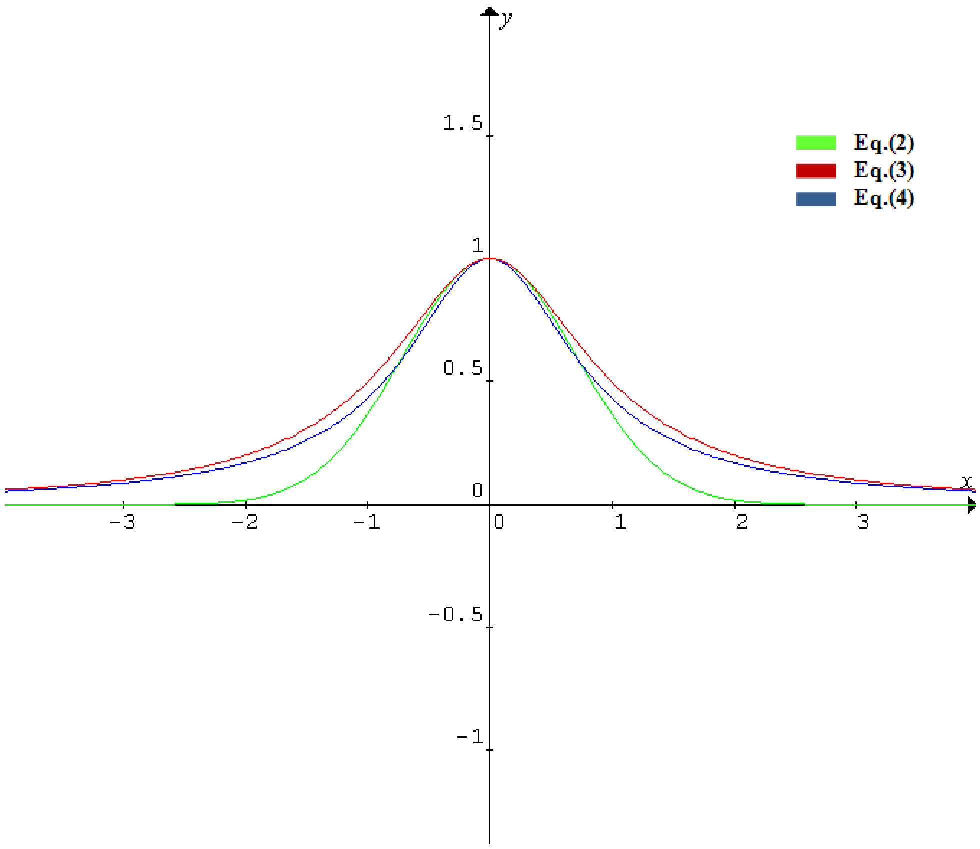

Figure 1. The New Diffusion Function

Through the above analysis on the strengths and weaknesses of P-M model diffusion function, this paper analyzes the principle of diffusion function smoothing that based on P-M model diffusion function, and proposes a new diffusion function, which can be used in the P-M model to maintain the advantages of original model , and greatly improve the speed of image smoothing[10]. This paper constructs the diffusion function as the Eq. (4):

$$g(x) = \frac{1}{\ln\left(e + \left(x/k\right)^2\right) + x^2} \tag{4}$$

New diffusion function is shown in Figure 1. Compared to the first two functions, the velocity being close to zero of new function is somewhere in between, which is more conducive to smoothing, de-noising, and edge-preserving.

2.2 Improvement of GGAC Model

GGAC is an improvement based on geodesic active contour model (GAC). There exists a serious deficiency in GAC, which may cause contraction curve to converge into certain local minimum value, as shown in Figure 2 [3].

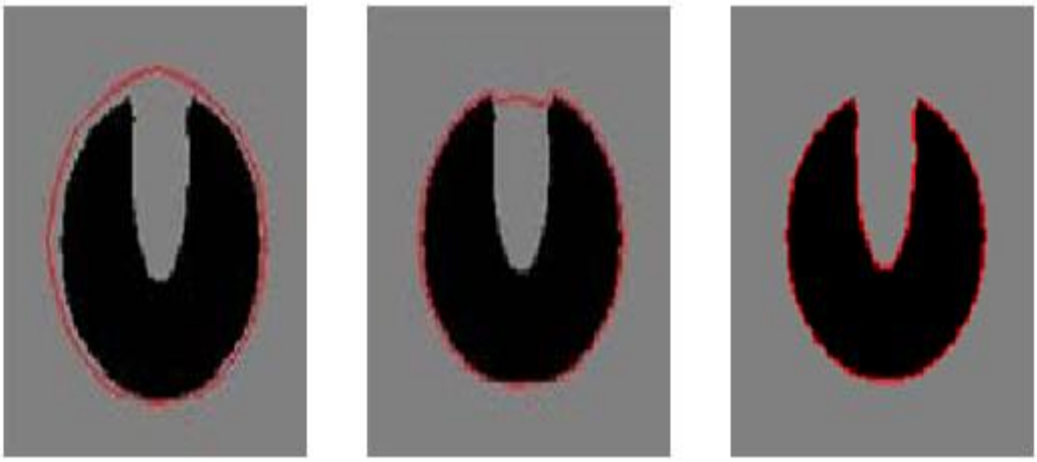

(a) The Original Image (b) The Result of GAC (c) The Result of GGAC

Figure 2. Segmentation Results Comparison of GAC Model and GGAC Model

GGAC has overcome this problem. In GGAC model, it introduces a contractile force item, hence the corresponding gradient descent flow is expressed as Eq. (5) [3]:

$$C_t = g(|\nabla I|)(c + k)N - (\nabla g(\nabla I) \bullet N)N \tag{5}$$

This paper improves the gradient magnitude calculation method of GGAC, and improves its robustness to noise. Gray scale image is defined as $I(x, y)$. If the image is calculated directly, it will be affected by the noise, so this paper first conducts pre-smoothing images, as shown in Eq. (6) [3]:

$$I_\sigma(x, y) = I(x, y) * G_\sigma(x, y) \tag{6}$$

In Eq. (6) $I * G_\sigma$ is the Gaussian convolution of original image, and σ is the standard deviation of the Gaussian function. Common gradient amplitude calculation method is susceptible to the interference from noise, especially in the case of blurred edge[11]. In order to mitigate the effects of noise, this paper uses the gradient magnitude calculation method in Eq. (7):

$$\left|\nabla I(i,j)\right| = \frac{1}{4}\sqrt{\left|\nabla I_1(x,y)\right|^2 + \left|\nabla I_2(x,y)\right|^2 + \ldots + \left|\nabla I_7(x,y)\right|^2 + \left|\nabla I_8(x,y)\right|^2} \quad (7)$$

Here,
$\nabla I_1(i,j) = I(i-1, j+1) - I(i,j)$,
$\nabla I_2(i,j) = I(i, j+1) - I(i,j)$, … , $\nabla I_8(i,j) = I(i-1, j) - I(i,j)$.

$$G = \begin{bmatrix} a_1 & a_2 & a_3 \\ a_8 & [i, j] & a_4 \\ a_7 & a_6 & a_5 \end{bmatrix} \quad (8)$$

Eq. (7) uses the gradient average of eight directions to replace the gradient average of two directions; the positional relationship is shown in Eq. (8), which appears more robust to the noise appearance.

In the improved GGAC model, the new edge function selected in the paper is shown as Eq. (9):

$$g(\mathrm{r}) = \frac{1}{\ln\left(e + \left(r/k\right)^2\right) + r^2} \quad (9)$$

Where k is a selected constant, which can control the decline rate of g.

GGAC model can effectively avoid failure to accurately detect recessed boundary appearing in GAC model. However, it still has some limitations. To the images with no apparent rounded edges and clear texture features, it cannot accurately segment. To solve the above defects, this paper has proposed an edge detection method based on Canny operator and GGAC model of reaction-diffusion equation.

3. Combination Mode of Canny Operators and GGAC Model

3.1. Reconstruction of Boundary Stopping Function

Combination mode of Canny operators and GGAC model is mainly the reconstruction of stopping function [5]. GGAC model mainly utilizes the boundary stopping function g to segment the images, hence the structure of g directly affects the result of the segmentation. However, no matter how to take the boundary stopping function, GGAC model itself still cannot accurately segment the images with the weak boundary or inconspicuous texture image. Instead, Canny operator has a very good edge extraction effect, so these two methods could complement each other. The author first uses Canny operator to detect image edge, and takes the detection result as the judgment conditions of GGAC model boundary for stop function g, hence the implementation of the reconstruction of boundary stopping function g. In this case, the boundary stopping function reconstruction is reconstructed as Eq. (10):

$$g'(r) = \begin{cases} \dfrac{1}{\ln\left(e + \left(r/k\right)^2\right) + r^2} & (m\ (\mathrm{i},\ \mathrm{j}) = 0) \\ \approx 0 & (m\ (\mathrm{i},\ \mathrm{j}) = 1) \end{cases} \quad (10)$$

Here, m is assumed to be edge detection result of Canny operator. For any point in the image, when $m(\mathrm{i,\ j}) = 1$, this point is edge point; when $m(\mathrm{i,\ j}) = 0$, the point is non-edge point of the image.

3.2. Numerical Implementation by Using the Improved Variational Level Set Method

The procedures using the combination mode of Canny operator and GGAC model for segmentation are[12]:

Step 1: Process with Canny operator, and the edge detection result is m.

Step 2: Calculate the gradient modulo value of target area image, and introduce gradient modulo value from each pixel into r to calculate edge function g.

Step 3: Use improved variational level set for numerical realization.

According to Eq. (5), the below Eq. (11) is obtained[6]:

$$\beta = g(k + c) - \nabla g \bullet N \tag{11}$$

Where, β is the statutory rate. PDE of embedding function u corresponding to Eq. (11) is[6]:

$$\frac{\partial u}{\partial t} = \beta|\nabla u| = \left[g(k + c) + \nabla g \bullet \frac{\nabla u}{|\nabla u|} \right] |\nabla u| = cg|\nabla u| + div\left(g\frac{\nabla u}{|\nabla u|} \right)|\nabla u| \tag{12}$$

Discretize the divergence operator $div()$ in Eq. (12), adopt the “semi-discretization”, and obtain Eq. (13) [6]:

$$\begin{aligned} div\left(g\frac{\nabla u}{|\nabla u|} \right) \approx\; & g_{i,j+1/2}\left(\frac{u_x}{|\nabla u|} \right)_{i,j+1/2} - g_{i,j-1/2}\left(\frac{u_x}{|\nabla u|} \right)_{i,j-1/2} \\ & + g_{i+1/2,j}\left(\frac{u_x}{|\nabla u|} \right)_{i+1/2,j} - g_{i-1/2,j}\left(\frac{u_x}{|\nabla u|} \right)_{i-1/2,j} \end{aligned} \tag{13}$$

The improved variational level set method just add a forced entry[13] that maintains the embedding function as distance function in the "energy" Pan function (13), hence[6]:

$$E(u) = \mu\iint_{\Omega} (|\nabla u| - 1)^2 dxdy + \iint_{\Omega} g|\nabla H(u)|dxdy + c\iint_{\Omega} [1 - H(u)]gdxdy \tag{14}$$

It corresponds to the gradient descent flow[6]:

$$\frac{\partial u}{\partial t} = \mu\left[\Delta u - div\left(\frac{\nabla u}{|\nabla u|} \right) \right] + \delta_{\varepsilon}(u)\left[div\left(g\frac{\nabla u}{|\nabla u|} \right) + cg \right] \tag{15}$$

Where, the discretization of Δu can be obtained by using a simple “4-neighbor-point” difference scheme (16) [6]:

$$(\Delta u)_{i,j} = u_{i+1,j} + u_{i-1,j} + u_{i,j+1} + u_{i,j-1} - 4u_{i,j} \tag{16}$$

Parameter μ is used to control the relative size of the role that forced action. When $\tau\mu \leq 0.25$, the display program of Eq.(15) is stable, so it is necessary to combine the μ selection the selection with τ [6-14].

The improved variational level set method has the advantages of higher stability and flexibility in selecting the time step according to the actual situation in the explicit program. Furthermore, since the Canny operator has locked the edge of target region, this paper combine the GGAC model to further segment the target, which can reduce the evolution time and ensure the accuracy of segmentation.

4. Experimental Results and Discussion

In this paper, experimental platform is the PC with Windows XP operating system (Intel D820 CPU/4GB). The author has used Matelab7.0 to conduct comparative experiments on five typical wood surface defect images.

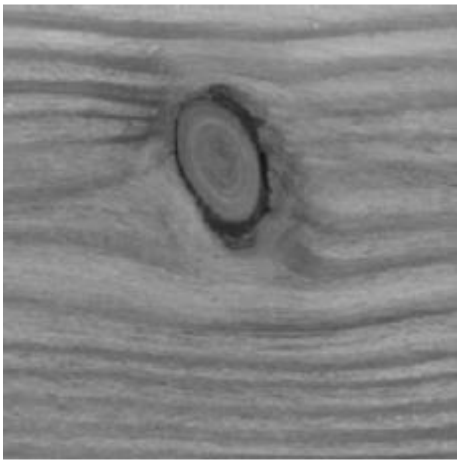

(a) Original Image of Dead-Knot Wood

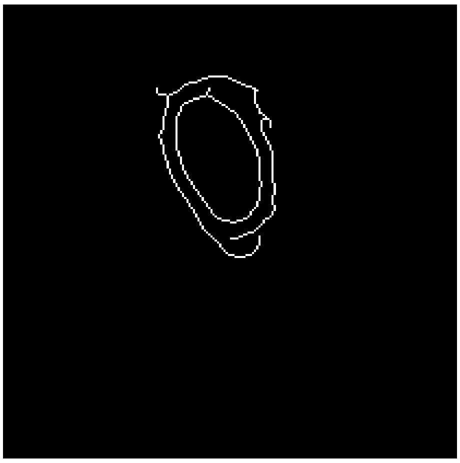

(b) The Improved Canny Operator

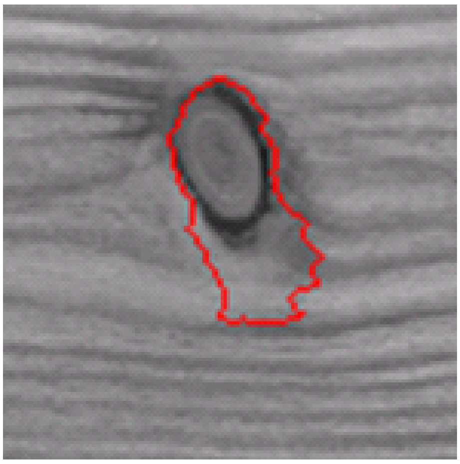

(c) Segmentation Results of Traditional GGAC

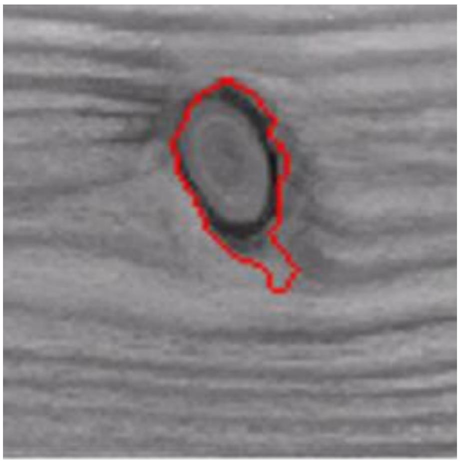

(d) The Improved Method

Figure 3. Comparison of Segmentation Results for Dead-Knot Image of the Wood Surface Defect

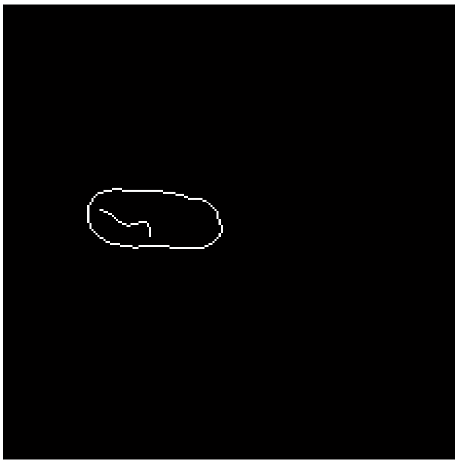

(a) Original Image of Worm Holes Wood (b) The Improved Canny Operator

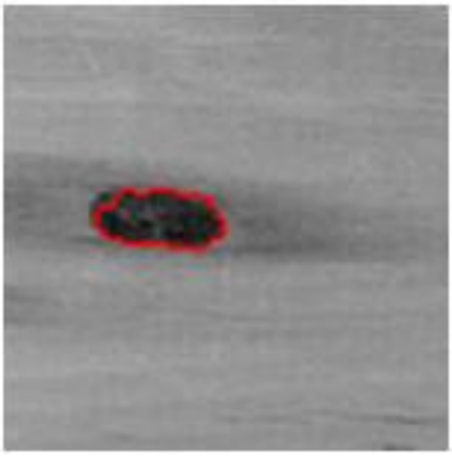

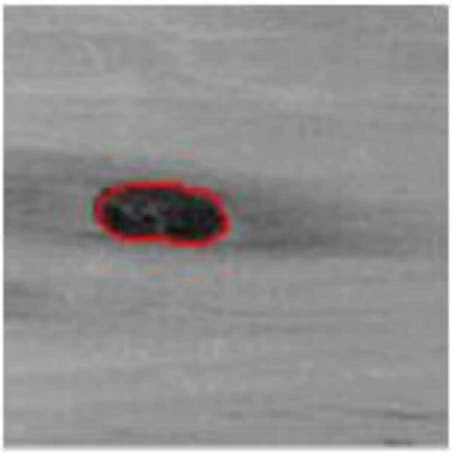

(c) Segmentation results of traditional GGAC (d) The Improved Method

Figure 4. Comparison of Segmentation Results for Worm Holes Image of the Wood Surface Defect

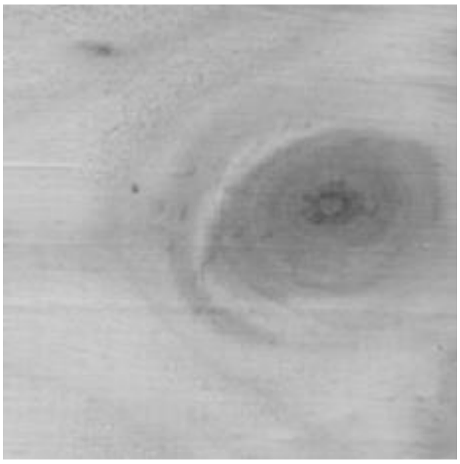

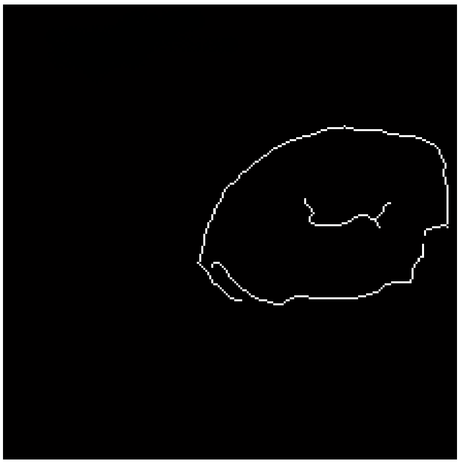

(a) Original Image of Slip-Knot Wood (b) The Improved Canny Perator

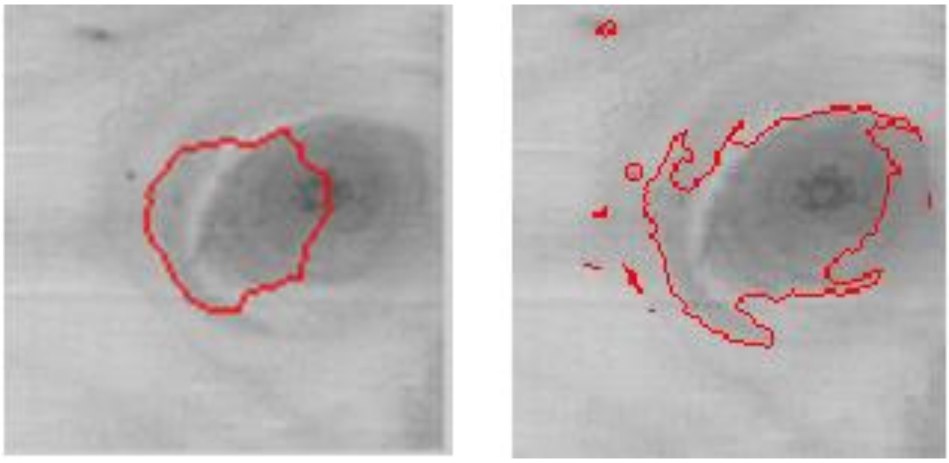

(c) Segmentation Results of Traditional GGAC (d) The Improved Method

Figure 5. Comparison of Segmentation Results for Slip-Knot Image of the Wood Surface Defect

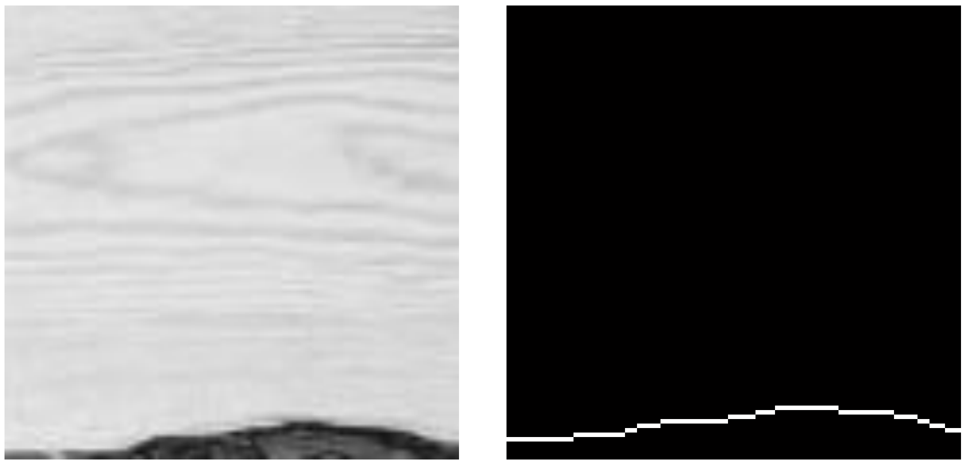

(a) Original Image of Edge-Missing Wood (b) The Improved Canny Operator

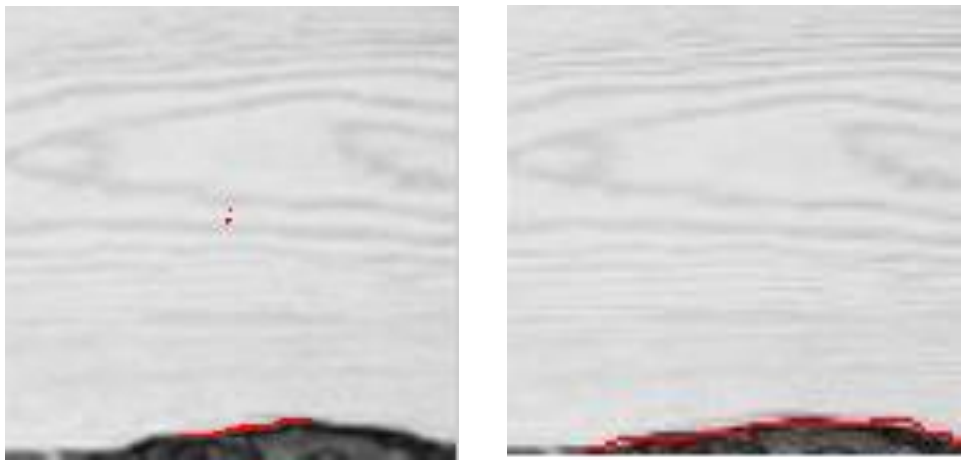

(c) Segmentation Results of Traditional GGAC (d) The Improved Method

Figure 6. Comparison of Segmentation Results for Edge-Missing Image of the Wood Surface Defect

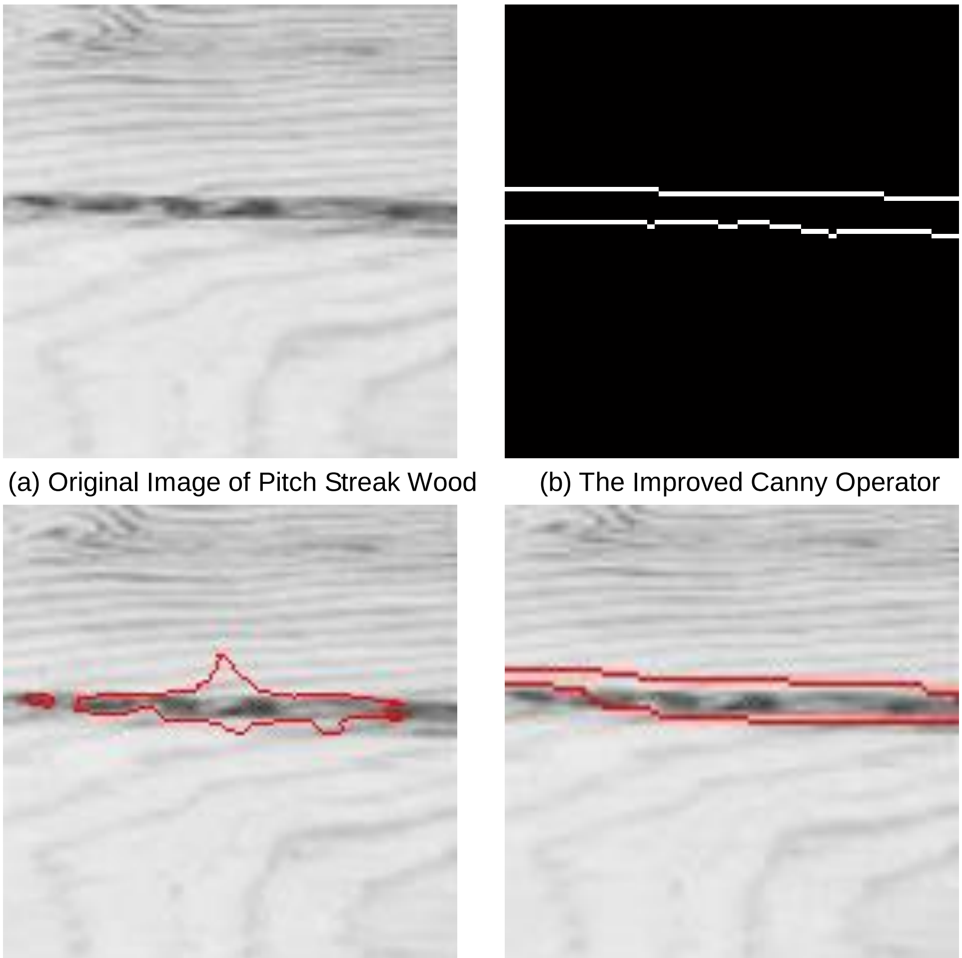

(a) Original Image of Pitch Streak Wood (b) The Improved Canny Operator

(c) Segmentation Results of Traditional GGAC (d) The Improved Method

Figure 7. Comparison of Segmentation Results for Pitch Streak Image of the Wood Surface Defect

In the experiment, the k=10 was taken [8]. The experiment respectively uses dead-knot image, slipknot image, wormhole image, edge-missing image and pitch streak image [15]. All the images are 128x128 pixels.

As shown, Figure 3 is the comparison of segmentation results for dead-knot image of the wood surface defect. Figure 4, shows the comparison of segmentation results for wormhole image of the wood surface defect. Figure 5, is the comparison of segmentation results for slipknot image of the wood surface defect, Figure 6, is the comparison of segmentation results for edge-missing image of the wood surface defect, and Figure 7, is the comparison of segmentation results for pitch streak image of the wood surface defect. According to the segmentation results, wood surface defect images segmentation method based on Canny operator and GGAC model combination, has achieved better segmentation results on images with dramatic changes of gray scale, such as worm holes, dead knots, edge-missing, pitch streak types, and it also well segmented on the types of weak boundary defects images, such as slip knot image that does not have obvious gray value transition with surrounding normal wood tissue.

5. Conclusions

For the segmentation of wood surface defect images, especially the wood surface with a weak edge, this paper presents an effective method. First, the paper improves the GGAC model and Canny operator respectively, and then combines with the two methods.

Compared with traditional GGAC model segmentation method and Canny operator edge detection algorithm, this method has the advantages of high reliability, good continuity, and high accuracy. It could not only achieve good results on the general wood surface defect images, but also have a very satisfactory effect on the wood surface defect images segmentation with weak edge. This method is not only an extension of the method for the segmentation of wood surface defects, but also extends the use of GGAC and Canny operators.

References

[1] L. Wang and X. B. Bai, "Image Segmentation method of surface defects of wood based on Gabor transform", Computer engineering and design, vol. 05, **(2010)**, pp. 1066-1069.
[2] X. B. Bai, "Image segmentation of wood surface defect based on Markov random field", Forestry science and technology, vol. 04, **(2013)**, pp. 33-36.
[3] J. Yuan, P. Li and Y. Wen, "Border segmentation using an improved GGAC model with points distance and gray intensity", International conference on multimedia technology, **(2010)**, pp. 1-5.
[4] L. Chen, "The segmentation of timber defects based on color and the mathematical morphology", Optik - International Journal for Light and Electron Optics, vol. 125, **(2014)**, no. 3.
[5] J. S. Shen, "A Water edge extraction method from Image based on Canny operator and GAC model", Journal of Surveying and Mapping Science and technology, no. 3, **(2013)**, pp. 264-268.
[6] D. K. Wang, "Partial differential equation method for image processing", Science Press, Beijing, **(2008)**.
[7] J. Canny, "A Computational Approach to Edge Detection", IEEE Trans. Pattern Anal. Mach. Intell., , vol. 8 **(1986)**.
[8] P. Perona and J. Malik, "Scale-Space and Edge Detection Using Anisotropic Diffusion", IEEE Trans, Pattern Anal. Mach. Intell., vol. 12, **(1990)**.
[9] K. Karantzalos and D. Argialas, "Improving edge detection and watershed segmentation with anisotropic diffusion and morphological levellings", International Journal of Remote Sensing, vol. 27, no. 24, **(2006)**.
[10] C. C. Leng, "Improved diffusion function of P-M model", Computer and modernization, **(2008)**, no. 01, pp. 19-20-23.
[11] X. M. Pardo, "A snake for CT image segmentation integrating region and edge information", Image and Vision Computing, vol. 19, no. 7, **(2001)**.
[12] Z. Ren and S. Das, "Variational Level Set Method for Two-Stage Image Segmentation Based on Morphological Gradients", Mathematical Problems in Engineering, **(2014)**.
[13] M. M. Abdelsamea, G. Gnecco and M. M. Gaber, "An efficient Self-Organizing Active Contour model for image segmentation", Neurocomputing, **(2014)**.
[14] Y. Yuan and C. He, "Variational level set methods for image segmentation based on both L 2 and Sobolev gradients", Nonlinear Analysis: Real World Applications, vol. 13, no. 2, **(2011).**
[15] X. B. Bai, "Application study of GVF Snake model in wood surface defects segmentation", Journal of Central South University of Forestry and Technology, vol. 02, pp. 90-95, **(2015)**.

Authors

Zhang Xianhong, Female. Date of Birth: 1.19.1983. Native Place: Harbin, China. Health: Good. Education: 2002.9-2006.6 Harbin College, Bachelor: 2006.9-2009.6, Harbin Normal University, Master. The majors are all computer application technology.

Zhang Chunrui, Female .Professor, received her PhD degree in mathematics from Harbin Institute of Technology. She is a professor of the Department of Mathematics, Northeast Forestry University. Her current research interests include Differential Equation, Dynamical Systems and Mathematical Biology.